11

Ultrafast Heating Characteristics in Multi-Layer Metal Film Assembly Under Femtosecond Laser Pulses Irradiation

Feng Chen, Guangqing Du, Qing Yang, Jinhai Si and Hun Hou
Xi'an Jiaotong University, School of Electronics and Information Engineering
China

1. Introduction

In recent years, ultrashort pulsed laser micromachining of multi-layer metal film assembly had attracted great attention because the multi-layer configuration can be well applied for satisfaction of thermal, optical and electronic requirements in development of MEMs, photoelectric equipments and biochips (Liu, 2007). Generally, the thermal properties for metals are physically originated from the collision mechanisms for electron-electron and electron-phonon in the metal targets. For the multi-layer metal film assembly, the thermal properties, such as the electron-phonon coupling strength can actually vary significantly for different layers of the assembly, so the heating of muti-layer film assembly would take on various characteristics for different padding layer configurations. In this article, the ultrafast heating characteristics in multi-layer metal film assemblies irradiated by femtosecond laser pulse were investigated by numerical simulations. The effect of different padding layer configurations on the ultrafast thermalization characteristics for the multi-layer metal film assemblies are well discussed. The ultrafast heat transfer processes in the layered metal film systems after the femtosecond pulse excitation are described based on the two temperature model (TTM), in which the electron and phonon is considered at two different temperatures, and heat transfer is mainly due to the hot electron diffusion among the sub-electron system and the electron energy transfer to the local lattice characterized by the electron-phonon coupling strength. The thermal properties for the respective metal film layers and the optical surface reflectivity are all defined as temperature dependent parameters in order to well explore the ultrafast heating characrastics of the multi-layer metal assemblies. The coupling two temperature equations are calculated by the Finite Element Method (FEM) with respect to temperature dependent thermal and optical properties. The ultrafast two-dimension (2-D) temperature field evolutions for electron and phonon subsystems in the multi-layer metal film assemblies are obtained, which show that the electron and phonon temperature field distributions can be largely effected by adjusting padding layer configurations. The physical origins for the discrepant temperature field distributions in multi-layer film assemblies are analyzed in details. It indicates that electron-phonon coupling strength and phonon thermal capacity play key roles in determining the temperature field distributions of the multi-layer film assembly.

2. Modelling and methods

2.1 Mathematical model

For pulsed laser ablation of metals, the ultrafast heating mechanisms perform great disparity for femtosecond and nanosecond pulse duration. In fact, the electron and phonon thermally relax in harmony for the nanosecond laser ablation, however, which are out of equilibrium severely for femtosecond laser ablation due to the femtosecond pulse duration is quite shorter compared to the electron–phonon relaxation time. So, it is expected that the basic theory for describing the femtosecond laser pulses interactions with metal is quite different from that of nanosecond laser pulses. In general, for femtosecond laser pulses, the heating involves high-rate heat flow from electrons to lattices in the picosecond domains. The ultrafast heating processes for femtosecond pulse interaction with metals are mainly consist two steps: the first stage is the absorption of laser energy through photon–electron coupling within the femtosecond pulse duration, which takes a few femtoseconds for electrons to reestablish the Fermi distribution meanwhile the metal lattice keep undisturbed. The second stage is the energy distribution to the lattice through electron–phonon coupling, typically on the order of tens of picoseconds until the electron and phonon reaches the thermal equilibrium. The different heating processes for electron and phonon were first evaluated theoretically in 1957 (Kaganov et al.,1957). Later, Anisimov et al. proposed a Parabolic Two Temperature Model (PTTM), in which the electron and phonon temperatures can be well characterized (Anisimov et al.,1974). By removing the assumptions that regard instantaneous laser energy deposition and diffusion, a Hyperbolic Two Temperature Model (HTTM) based on the Boltzmann transport equation was rigorously derived by Qiu (Qiu et al.,1993). Further, Chen and Beraun extended the conventional hyperbolic two temperature model and educed a more general version of the Dual-Hyperbolic Two Temperature Model (DHTTM), in which the electron and phonon thermal flux are all taken into account (Chen et al., 2001). The DHTTM has been well applied in the investigation of ultrashort laser pulse interaction with materials. The mathematical models for describing the DHTTM can be represented in the following coupling partial differential equations:

$$C_e \frac{\partial T_e}{\partial t} = -\nabla q_e - G(T_e - T_p) + Q \tag{1}$$

$$C_p \frac{\partial T_p}{\partial t} = -\nabla q_p + G(T_e - T_p) \tag{2}$$

where subscripts e and p stands for electron and phonon, respectively. T denotes temperature, C the heat capacity, q the heat flux, G the electron-phonon coupling strength, and Q is the laser heat source. The first equation describes the laser energy absorption by electron sub-system, electrons thermal diffusion and electrons heat coupling into localized phonons. The second equation is for the phonon heating due to coupling with electron sub-system. For metal targets, the heat conductivity in phonon subsystem is small compared to that for the electrons so that the phonon heat flux q_p in Eq.(2) can be usually neglected. The heat flux terms in Eq.(1) with respect to the hyperbolic effect can be written as

$$q_e = -(k_e \nabla T_e + \tau_e \partial q_e / \partial t) \tag{3}$$

here k_e and τ_e denotes the electron heat conductivity and the electron thermal relaxation time. Further, letting the electron thermal relaxation time τ_e be zero. Consequently the DHTTM can be reduced to the Parabolic Two Temperature Model (PTTM), which had been widely used for investigation of the ultrashort laser pulse interaction with metal films.
For the multi-layered metal film assembly, the PTTM can be modified from Eqs.(1)-(3) and written as the following form for the respective layers:

$$C_e^{(i)} \frac{\partial T_e^{(i)}}{\partial t} = -\nabla q_e^{(i)} - G(T_e^{(i)} - T_p^{(i)}) + Q^{(1)} \tag{4}$$

$$C_p^{(i)} \frac{\partial T_p^{(i)}}{\partial t} = G^{(i)} \left(T_e^{(i)} - T_p^{(i)} \right) \tag{5}$$

where $q_e^{(i)}$ is the heat flux vector, described as $-k_e^{(i)} \nabla T_e^{(i)}$. The superscript i relates to the layer number in the multi-layer assembly. The laser heat source term is usually considered as Gaussian shapes in time and space, which can be written as

$$Q^{(1)} = S(x,y) \cdot T(t) \tag{6}$$

where

$$S(x,y) = \sqrt{\frac{4\ln 2}{\pi}} \frac{1-R}{t_p(\delta + \delta_b)} F \times \exp\left[-\frac{x}{\delta + \delta_b} - \left(\frac{y - y_0}{y_s} \right)^2 \right] \tag{7}$$

$$T(t) = \exp\left(-4\ln 2 \left(\frac{t - 2t_p}{t_p} \right)^2 \right) \tag{8}$$

here, R is the film surface reflectivity, t_p is the FWHM (full width at half maximum) pulse duration, $\delta + \delta_b$ is defined as the effective laser penetration depth with δ and δ_b denoting the optical penetration depth and electron ballistic range, respectively. F is the laser fluence. y_0 is the coordinate of central spot of light front at the plane of incidence and y_s is the profile parameter. When a laser pulse is incident on metal surface, the laser energy is first absorbed by the free electrons within optical skin depth. Then, the excited electrons is further heated by two different processes, which includes the thermal diffusion due to electron collisions and the ballistic motion of excited electrons. So, we use the effective laser penetration depth in order to account for the effect of ballistic motion of the excited electrons that make laser energy penetrating into deeper bulk of a material.

2.2 Initial and boundary conditions

The calculation starts at time *t*=0. The electrons and phonons for the respective layers in the multi-layer film systems are assumed to be room temperature at 300 K before laser pulse irradiation. Thus, the initial conditions for the multi-layer metal film assembly are:

$$T_e^{(1)}(t=0) = T_e^{(2)}(t=0) = \cdots = T_e^{(i)}(t=0) = 300\text{K} \tag{9}$$

$$T_p^{(1)}(t=0)=T_p^{(2)}(t=0)=\cdots=T_p^{(i)}(t=0)=300\text{K} \tag{10}$$

For the exterior boundaries of the multi-layer assembly, it is reasonable to assume that heat losses from the metal film to the surrounding as well as to the front surface are neglected during the femtosecond-to-picosecond time period. The perfect thermal insulation condition between bottom layer of assembly with the substrate can also be established at rear surface of the multi-layer film assembly. Therefore, the exterior boundary conditions can be written as:

$$\frac{\partial T_e}{\partial n}\Big|_{\Omega}=\frac{\partial T_p}{\partial n}\Big|_{\Omega}=0 \tag{11}$$

here, Ω represents the four borderlines of the 2-D metal film assembly.
For the interior interfaces of the multi-layer systems, we assume the perfect thermal contacts for electron subsystem between the respective layers herein, leading to

$$T_e^{(1)}\Big|_{\Gamma}=T_e^{(2)}\Big|_{\Gamma}=\cdots=T_e^{(i)}\Big|_{\Gamma} \tag{12}$$

$$q_e^{(1)}\Big|_{\Gamma}=q_e^{(2)}\Big|_{\Gamma}=\cdots q_e^{(i)}\Big|_{\Gamma} \tag{13}$$

where, Γ represents the interior interfaces of the multi-layer assembly. Additionally, the phonon thermal transfer at layer interface is considered to be impracticable due to the small phonon heat conductivity during the picosecond timescale. So, the phonon temperature and thermal flux are all treated as discontinuous physical quantities at the layer interfaces of the multi-layer film assemblies in current simulations.

2.3 Temperature dependent thermal properties

Most of the previous researches considered the thermal parameters for gold film as constant values for simplification of the calculations and saving the computer time. Herein we treat all the thermal properties including thermal capacity, thermal conductivity and the electron-phonon coupling strength as temperature dependent parameters in order to well explore the heating characteristics in the metal films assembly under ultrashort laser pulse irradiation. According to the Sommerfeld theory, electron thermal conductivity at low temperature is given in paper (Christensen et al., 2007)

$$k_e=\frac{1}{3}v_F^2C_e'T_e\left(\frac{1}{\tau_{ee}}+\frac{1}{\tau_{ep}}\right) \tag{14}$$

where $1/\tau_{ee}=AT_e^2$ and $1/\tau_{ep}=BT_p$ is temperature dependent electron-electron and the electron-phonon scattering rates, with which the temperature dependent thermal conductivity can be educed. We assume that the electrons and phonons are isotropic across the target so that the isotropic thermal properties for the targets can be applied in the current simulations. In the regime of high electron temperature, the electron-electron interactions must be taken into account, leading to

$$k_{e1}=B_ek_{e,0}\frac{T_e}{A_eT_e^2+B_pT_p} \tag{15}$$

However, when the electron temperature is low enough that electron-electron interactions compared to electron-phonon collisions can be neglected, the electron thermal conductivity is written as

$$k_{e2} = k_{e,0}\, T_e / T_p \tag{16}$$

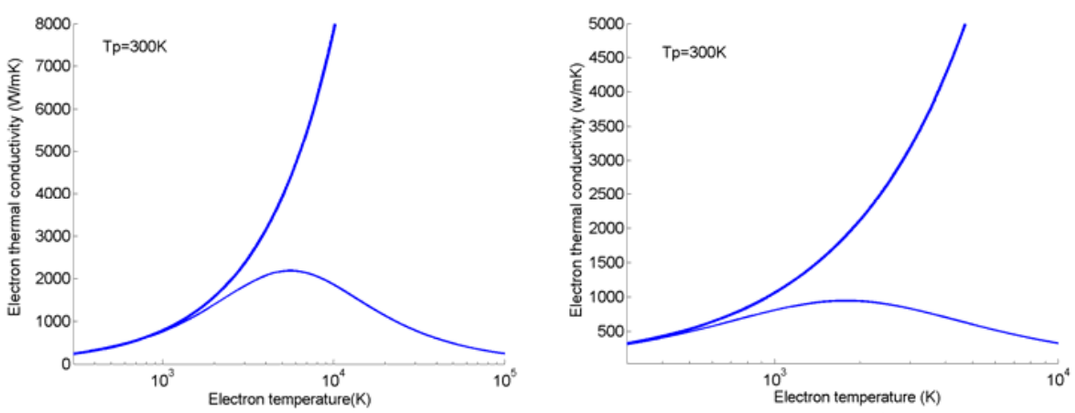

(a) (b)

Fig. 1. The electron thermal conductivity as a function of electron temperature for the targets of Au (a) and Al (b), the thick line stands for k_{e2}, the thin line stands for k_{e1}

The electron thermal conductivity as a function of electron temperature for the targets of Au and Al are shown in Fig.1. We can see that the electron thermal conductivity when ignoring the term of electron-electron collisions increases dramatically with increasing the electron temperature. However, as the electron-electron collisions term is taken into account, the thermal conductivity curve appears a peak approximately at the temperature of 5500 K for Au, and 1900 K for Al, and the peak thermal conductivity for Au is twice larger than for Al. It indicates that the effect of electron-electron collisions on the electron thermal conductivity is significant in the range of high electron temperature, but not exhibits large difference in low electron temperature regime.

The temperature dependent electron heat capacity is taken to be proportional to the electron temperature with a coefficient B_e (Kanavin et al.,1998):

$$C_e(T_e) = B_e T_e \tag{17}$$

An analytical expression for the electron-phonon coupling strength was proposed by Chen et. al., which can be represented as follows (Chen et al., 2006):

$$G(T_e, T_p) = G_0 \left[\frac{A_e}{B_p} (T_e + T_p) + 1 \right] \tag{18}$$

Fig.2 shows the electron-phonon coupling strength as a function of electron temperature for the targets of Au and Al. We fix the phonon temperature at room temperature of 300K. It is shown that the electron-phonon coupling strength increases obviously with increasing the electron temperature. It indicates that more electron energy can be transferred to localized

phonon due to the increase of electron-phonon coupling strength as a result of the rise of electron temperature. Meanwhile, the excited phonons sub-system also help strengthen the electron-phonon coupling process, leading to the further promotion of phonon temperature. It can be seen that the electron-phonon coupling strength is one order of magnitude larger for Al than Au in the temperature range of 300 K to 100000 K, which would result in the distinct phonon heating processes in the multi-layer metal film assembly for different layers.

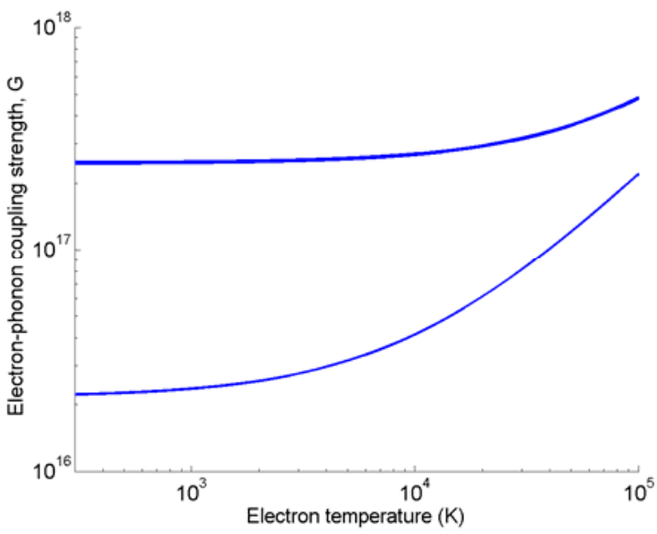

Fig. 2. The electron-phonon coupling strength as functions of electron temperature for Au and Al. The thick line stands for Al, the thin line stands for Au. The unit of G is J m^{-3} s^{-1} K^{-1}

2.4 Temperature dependent optical parameters

For femtosecond pulse heating of the metal film assembly, the electron sub-system for the surface layer can be initially heated to several thousand Kelvin during the pulse duration. So the effect of electron temperature on the optical properties such as the surface reflectivity should be carefully taken into account for accurately predicting the ultrafast electron and phonon heating processes in multi-layer metal film assemblies. The laser energy reflection from metal surface is physically originated to the particles collisions mechanisms including electron-electron and electron-phonon collisions in the target materials. For ultra-high non-equilibrium heating of the electron and phonon sub-systems under the femtosecond pulse excitation, the total scattering rates can be written as $v_m = A_e T^2 + B_b T_p$, in which the electron and phonon temperatures can jointly contribute to the total scattering rates. The connection between the metal surface reflectivity and the total scattering rate usually relates to the well-known Drude absorption model. After some derivations from Drude model, the reflective index n and absorptive coefficient k can be immediately written as:

$$n^2 = \frac{1}{2}\left[\left(1-\frac{\omega_p^2}{\omega^2+v_m^2}\right)^2+\left(\frac{v_m}{\omega}\frac{\omega_p^2}{\omega^2+v_m^2}\right)^2\right]^{\frac{1}{2}}+\frac{1}{2}\left(1-\frac{\omega_p^2}{\omega^2+v_m^2}\right) \tag{19}$$

$$k^2 = \frac{1}{2}\left[\left(1-\frac{\omega_p^2}{\omega^2+v_m^2}\right)^2+\left(\frac{v_m}{\omega}\frac{\omega_p^2}{\omega^2+v_m^2}\right)^2\right]^{\frac{1}{2}}-\frac{1}{2}\left(1-\frac{\omega_p^2}{\omega^2+v_m^2}\right) \tag{20}$$

where ω_p denotes the plasma frequency of the free electron sub-system, expressed as $\sqrt{e^2 n/\left(\varepsilon_0 m_e^*\right)}$, ω is the angular frequency of the laser field. Applying the Fresnel law at the surface, we can get the surface reflectivity coefficient:

$$R\left(T_e, T_p, \omega\right) = \frac{(n-1)^2+k^2}{(n+1)^2+k^2} \tag{21}$$

3. Results and discussion

Fig.3 shows the temporal evolution of electron and phonon temperature fields in the two layer Au/Ag film assembly. The laser is incident from left, the parameters for the laser pulse and the assembly are listed as follows: laser fluence F=0.1 J/cm², pulse duration t_p=65 fs, laser wavelength 800 nm, the thickness of padding layers $T_{Au} = T_{Ag} = 100\text{nm}$. Herein, the electron ballistic effect is included in the simulations. At time of 500 fs, the electron subsystem for the film assembly is dramatically heated, the maximal electron temperature at the front and rear surfaces of the two layer Au/Ag film assembly get 2955K and 1150K, respectively. However, the phonon subsystem for the bottom Ag film layer of the assembly is slightly heated at 500 fs, the phonon temperature field is mostly centralized at the first layer, approximately 20 nm under the Au film surface, the maximal phonon temperatures at front surface and the layer interface gets to 317K and 305K, respectively. At time of 1 ps, the electron temperature field penetrates into deeper region of the assembly, indicating that the electron heat conduction amongst electron subsystem is playing an important role during this period. The maximal electron temperature at the front surface drops down to 2100K and rises to 1500K at the rear surface. Simultaneously, the phonon temperature at the respective Au and Ag layers begins to rise, the maximal phonon temperatures at the front and the rear surfaces of the assembly climbs to 328 K and 313 K at 1ps. The bottom Ag layer phonon thermalization can actually be attributed to the electron thermal transfer from the first layer Au film to the Ag electron subsystem, and the following process in which the overheated electron coupling its energy to localized Ag film phonon subsystem through electron-phonon coupling. At time of 4ps, the electron temperature field is significantly weakened across the Au/Ag assembly and the phonon temperature fields are mostly distributed near the front surfaces of the respective Au and Ag layers at this time, the maximal phonon temperature at the front surface of the Au film and the Ag layer is 353.3 K and 345 K, respectively. With time, the electron and phonon subsystems ultimately would get the thermal equilibrium state and bears the united temperature distribution across the assembly. It should be emphasized that the temperature field distributions for electrons and phonons are quite different at the middle interface layer which is actually originated from the physical fact that phonon thermal flux can be ignored and electron presents excellent thermal conduction at the middle interface of the assembly during the picosecond time period.

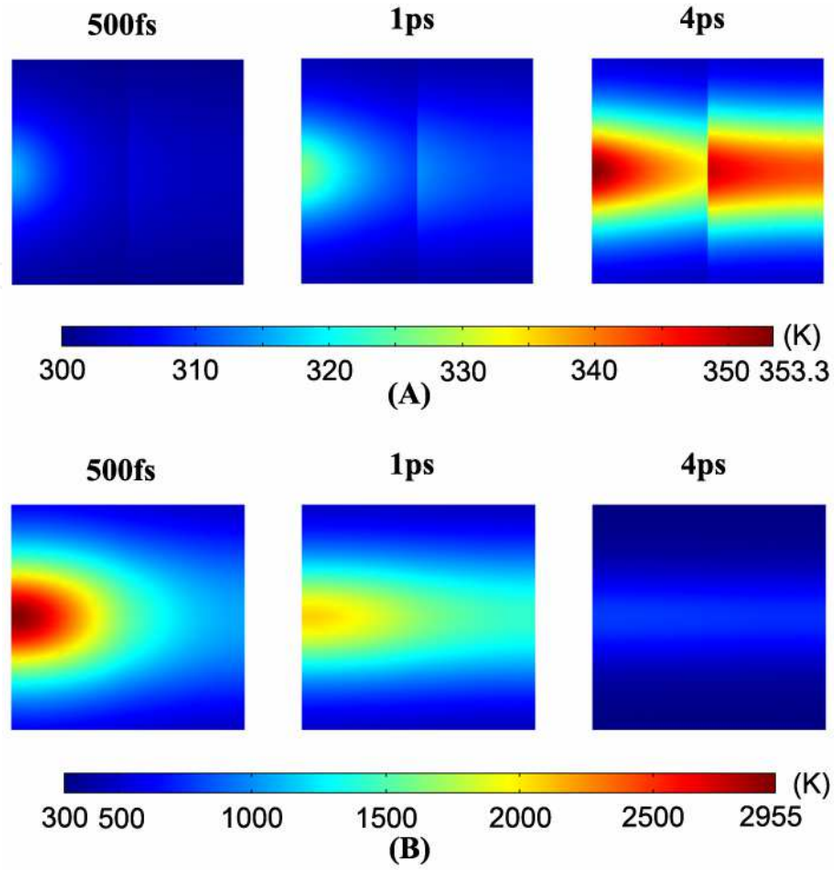

Fig. 3. The temporal evolution of electron and phonon temperature fields in two layer Au/Ag film assembly. (A) Phonon temperature fields at 500fs, 1ps and 4ps; (B) Electron temperature fields at 500 fs, 1ps and 4ps

Fig.4 shows the temporal evolution of electron and phonon temperature fields in the two layer Au/Al film assembly. The laser is incident from left, the laser pulse and the assembly parameters are listed as follows: laser fluence F=0.1 J/cm^2, pulse duration t_p= 65 fs, laser wavelength 800 nm, the thickness of padding layers T_{Au}=T_{Al}= 100 nm. It can be clearly seen from Fig.4(A) that the phonon temperature fields evolution for the Au/Al assembly exhibits different tendency as for the Au/Ag film assembly. At time of 500 fs, the surface Au layer phonon in the Au/Al film assembly is less heated, the deposited thermal energy is mainly concentrated at substrate Al layer. The maximal phonon temperature at front surface and middle interface of the assembly is 310 K and 330K, respectively. At time of 1ps, the phonon subsystem for the bottom Al layer is dominantly heated, while the surface Au layer phonon temperature keeps close to room temperature, the maximal phonon temperature at front surface and middle interface comes to 320K and 371 K at this time. Generally, the rapid rise of the bottom Al layer phonon temperature is primarily attributed to larger electron-phonon coupling strength for the Al layer compared to that of Au layer. The laser energy is firstly coupled into the electron of the surface Au layer, then the excited electron conducts it's energy to electron subsystem of bottom Al layer through electron thermal conduction. Immediately after that the Al layer electron couples it's energy to the local phonon, leading to preferential heating of the bottom Al film. At time of 4ps, the phonon subsystem of the Al

film is further heated and the phonon temperature at Au layer continues to rise very slowly, the maximal phonon temperature at front surface and the middle interface is 351K and 443K at this time. In Fig.4(B), the electron temperature field evolution for Au/Al film assembly dose not show significant difference from that of the Au/Ag film assembly. The electron subsystem of the two layer Au/Al film assembly is dramatically overheated at 500 fs, the maximal electron temperature at the front surface of the assembly reaches 2922 K. At time of 1ps, the electron subsystem continues diffusing it's thermal energy to the Al substrate, and the electron temperature for the surface Au film bears a severe drop. The maximal electron temperature comes down to 1900K at the front surface, and rises to 750K at the rear surface at 1ps. At time of 4ps, the electron temperature across the assembly goes down to 400K and 350K at front surface and rear surface, respectively. With time, the electron and phonon subsystems also would get the thermal equilibrium state, and if the united electron and phonon temperature in assembly is higher than padding layers melting point, the two layer film assembly will be damaged.

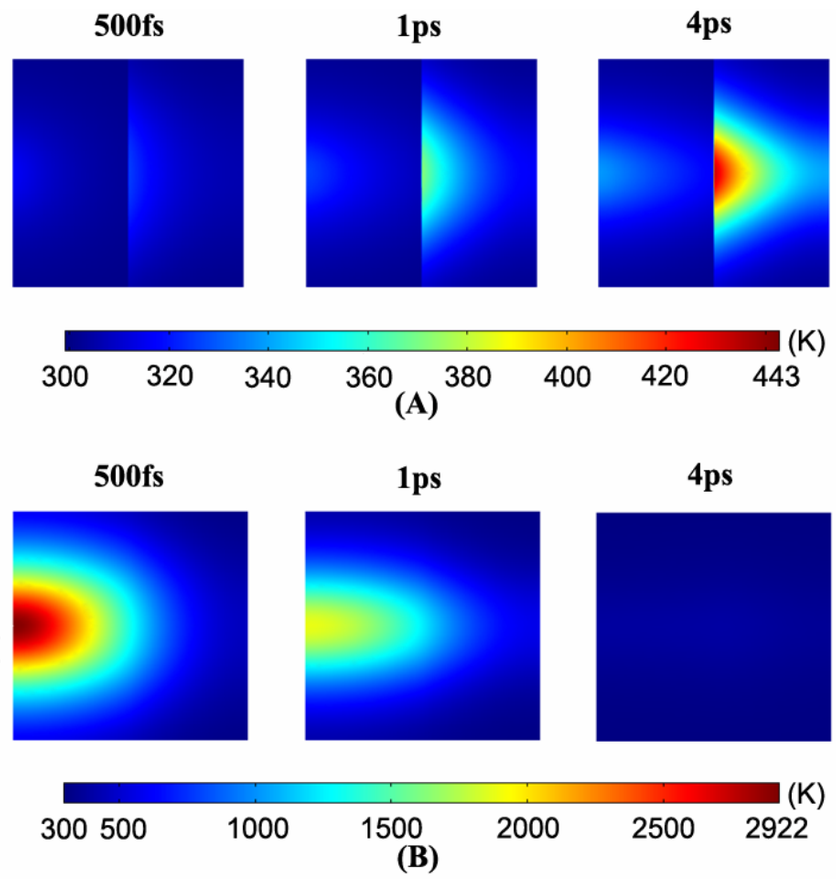

Fig. 4. The temporal evolution of electron and phonon temperature fields in two layer Au/Al film assembly. (A) Phonon temperature fields at 500fs, 1ps and 4ps; (B) Electron temperature fields at 500fs, 1ps and 4ps

Fig.5 presents the phonon temperature field distributions for the three layer film assemblies with different layer configurations at 5 ps. The laser and film parameters for the simulations are listed as follows: laser fluence is F=0.1 J/cm², pulse duration t_p=65 fs, laser wavelength

800 nm, the thicknesses of the respective padding layers are T_{Au}=T_{Ag}=T_{Al} =50 nm. The laser pulse is incident from left. It is shown in Fig.5 (A) that the phonon energy is concentrated at bottom of the assembly for Au/Ag/Al configuration, however, which is mostly distributed at the surface layer for Al/Ag/Au configuration as can be seen from Fig.5(B). The results can be partly interpreted as large electron-phonon coupling strength for Al compared to Au, which is beneficial for transferring the overheating surface electron thermal energy into the bottom layer phonon.

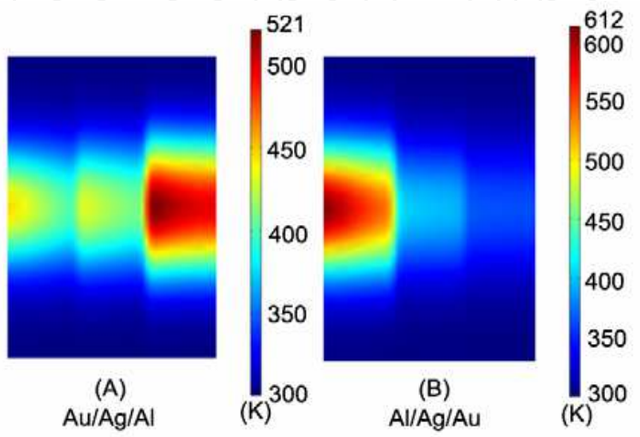

Fig. 5. The phonon temperature fields for three layer metal film assemblies with different layer configurations at time of 5 ps

The temporal evolution of surface phonon and electron temperatures at center of laser spot for Au coated assemblies with different substrates are shown in Fig.6. The applied thermal physical parameters for the substrates of Au, Ag, Cu and Al in the simulations are listed in table 1. As shown in Fig.6(a), the surface phonon temperature rises accordantly for the all assemblies before 1ps, then begins to separate for the different assemblies with increasing time. Finally, the surface phonon temperature gets 380K, 370K, 349K, and 386K at 15ps for assemblies of Au/Au, Au/Ag, Au/Cu and Au/Al, respectively. Fig.6(b) shows the surface electron temperature of the Au coated metals also evolutes synchronously before 1ps, but becomes discrepantly after 1 ps. It should be noticed that the surface phonon and electron temperatures at 15ps for the Au coated Al film substrate are obviously larger than that of the assemblies with other metal film substrates. It is expected that the thermal properties for the substrate layers can play an important role in enhancing surface temperature evolution on the Au coated metal assemblies.

Parameters	Au	Ag	Cu	Al
G_0(10^{16} J m^{-3} s^{-1} K^{-1})	2.1	3.1	10	24.5
C_{e0}(J m^{-3} K^{-2})	68	63	97	135
k_{e0}(J m^{-1} s^{-1} K^{-1})	318	428	401	235
C_l(10^6 J m^{-3} K^{-1})	2.5	2.5	3.5	0.244
A(10^7 s^{-1} K^{-2})	1.18	0.932	1.28	0.376
B(10^{11} s^{-1} K^{-1})	1.25	1.02	1.23	3.9

Table 1. Thermal physical parameters for Au, Ag, Cu and Al, the datum are cited from references (Chen et al., 2010 ; Wang et al., 2006)

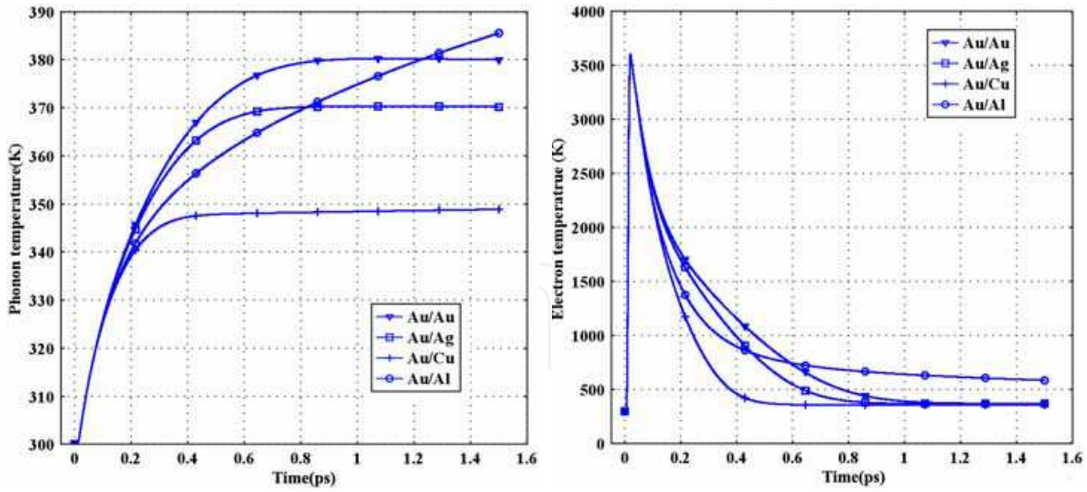

(a) Phonon temperature (b) Electron temperature

Fig. 6. Temporal evolution of phonon and electron temperatures at center of laser spot on surface of Au surfaced two layer metal film assemblies

In general, the physical mechanism in dominating the temperature field distributions has no difference for the two layer and the three layer metal film assemblies because of the similar physical boundary and the mathematical processing for them. So, the two layer Au coated metal assembly is here taken as example in order to explore what causes can definitely give rise to the distinct temperature field distributions in the metal film assembly with different substrate configurations? Fig.7 shows effect of the substrates thermal parameters on surface phonon temperature of the two layers Au coated assembly. The thermal parameters such as electron thermal capacity, electron thermal conductivity, electron-phonon coupling strength and phonon thermal capacity are all selected falling into the ranges for the actual materials as listed in table 1. As shown in Fig.7(a) and (b), the surface Au layer phonon temperature decreases slightly with increasing electron thermal capacity and electron thermal conductivity of the substrates. However, increasing of electron-phonon coupling strength or phonon thermal capacity for the substrate layers can both result in the dramatic drops of surface phonon temperature as shown in Fig.7(c) and (d), indicating the substrate layer electron-phonon coupling strength and phonon thermal capacity both play key roles in determining the surface heating process in the Au coated metal assembly. From table 1, it can be found out that the electron-phonon coupling strengths for the substrates is in the order of $G_{Au}<G_{Ag}<G_{Cu}$, so the surface Au phonon would be preferentially heated for Au/Au, Au/Ag, Au/Cu orderly as had be observed in Fig.6. However, the obvious rise of the Au surface phonon temperature for Au/Al assembly is actually attributed to the quite smaller phonon thermal capacity for the Al substrate compared to other metal substrates.

Fig.8 shows temporal evolution of electron and phonon temperature in the two layer Au/Al assembly at different depths. The laser parameters are t_p=65 fs, F=0.1 J/cm^2, wavelength is 800 nm. It can be seen from Fig.8(a) that when the depth exceeds 100 nm, the pulse-like distribution of electron temperature profile fades away, which can be related to the role of the electron ballistic effect. Beyond the ballistic range, taken as 100 nm here, the temporal information of laser pulse can less be delivered to the electron temperature for the Au/Al assembly. We can see from Fig.8(b) that the phonon temperature evolutions for the surface layer at depths of 0 nm and 50 nm is severely inhibited, however, which rises dramatically

at depths of 150 nm and 200 nm for the substrate layer. It indicates the phonon subsystem is heated in priority from substrate to the surface layer for the Au/Al assembly.

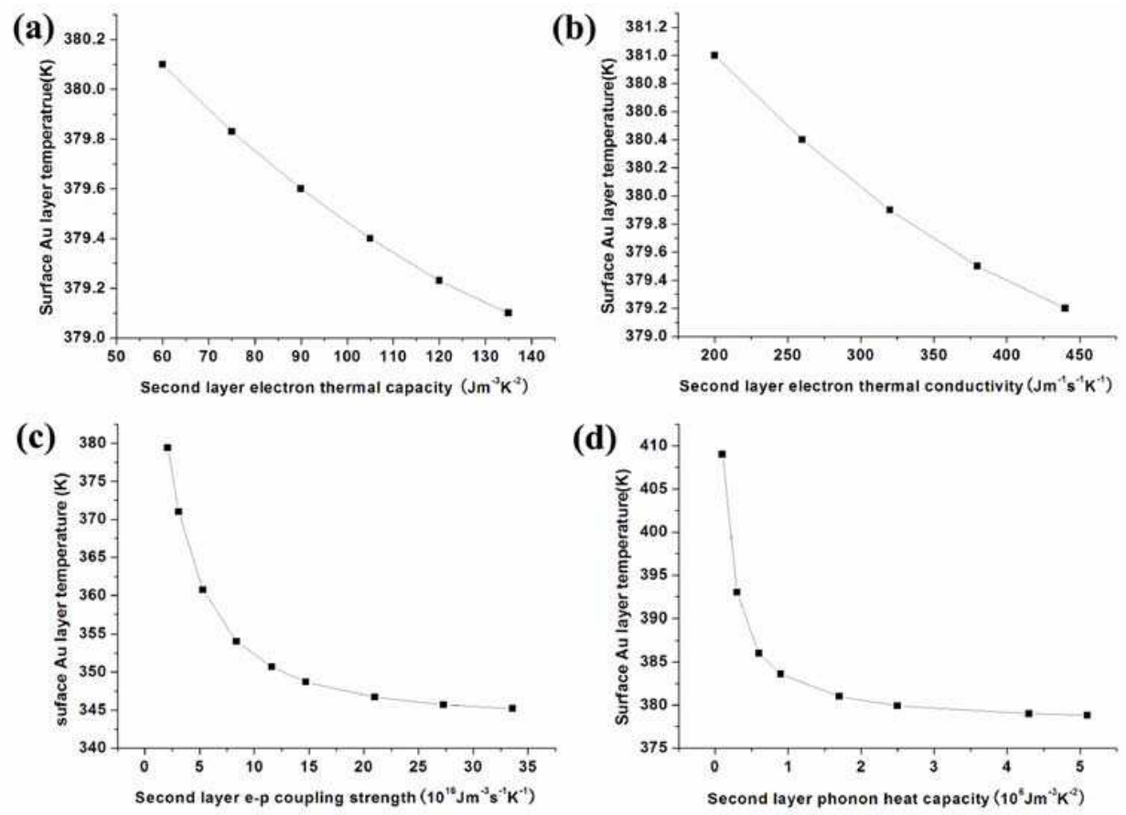

Fig. 7. Effect of thermal parameters of the substrate layer on surface phonon temperature of the two layer Au/substrate assembly

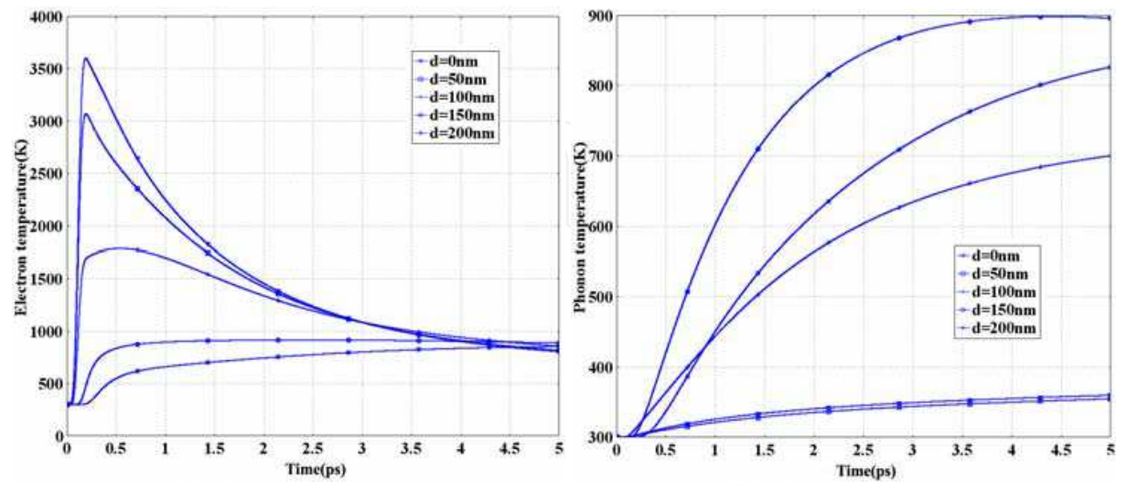

(a) Electron temperature (b) Phonon temperature

Fig. 8. Temporal evolutions of electron and phonon temperature for the Au/Al film assembly at different depths of the target

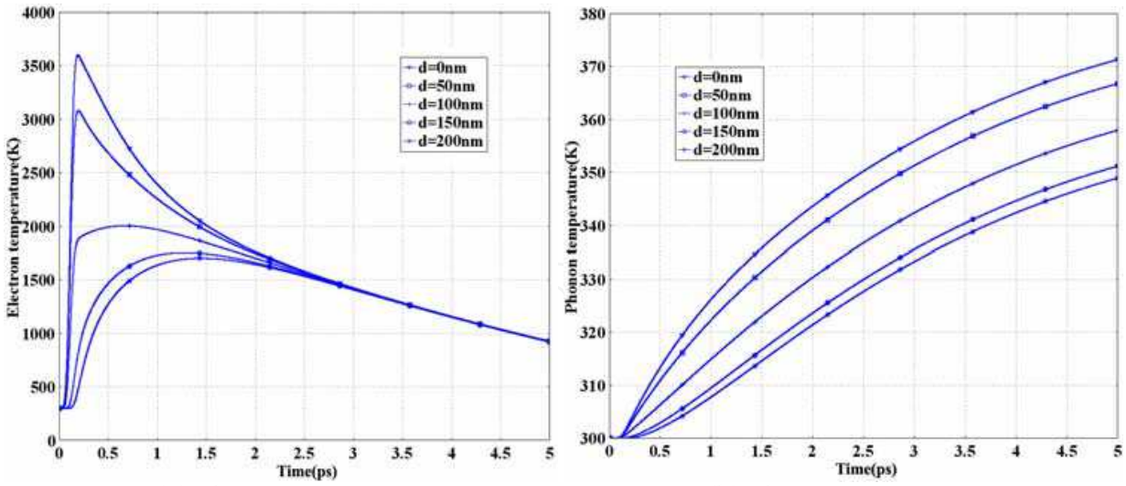

(a) Electron temperature (b) Phonon temperature

Fig. 9. Temporal evolution of electron and phonon temperature for the Au/Ag film assembly at different depths of the target

The temporal evolution of electron and phonon temperature for the Au/Ag film assembly at different depths of the target are given in Fig.9. The laser parameters are t_p=65 fs, F=0.1 J/cm^2, wavelength is 800 nm. As show in Fig.9(a), the electron temperature peak decreases orderly with increasing the depth. As the depth exceeds 100 nm, the electron temperature profile still maintains the pulse-like distribution, although the sharp pulse structure is weakened for the Au/Ag film assembly, which is different from that of the Au/Al film assembly. From Fig.9(b), it can be seen that the phonon temperature rises more rapidly from depths of d=0 nm to d=200 nm. In fact, the thermal parameters between Au and Ag is very close to each other so that the electron and phonon temperature evolutions in the Au/Ag assembly perform the normal tendency as usually found in single layer metal film heating, namely, the film is preferentially heated from surface to the bottom.

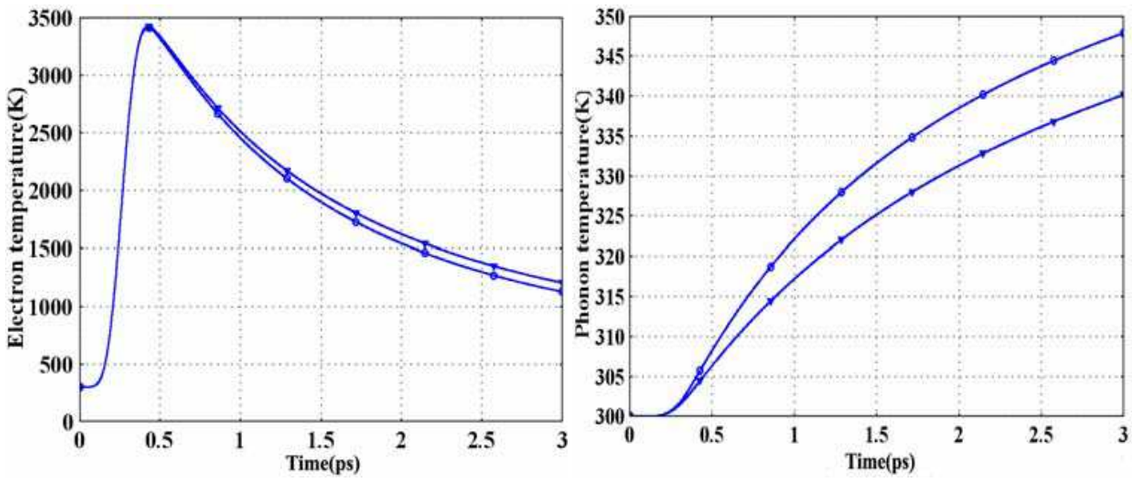

(a) Electron temperature (b) Phonon temperature

Fig. 10. The surface electron temperature of the two layer Au/Al film assembly at center of laser spot as a function of delay time. (The circle represents the temperature dependent electron-phonon coupling strength, and the triangle represents constant coupling strength)

Fig.10 shows surface electron and phonon temperatures of the two layer Au/Al assembly at center of laser spot as a function of delay time with respect to the temperature dependent and constant electron-phonon coupling strengths. The laser parameters are t_p=150 fs, F=0.1 J/cm^2, laser wavelength is 800 nm. The temporal evolutions of electron and phonon temperatures are almost identical during the femtosecond laser pulse duration and becomes discrepantly after 300 fs. The simulated electron temperature using temperature dependent electron-phonon coupling strength is slightly lower compared to that applying the constant electron-phonon coupling strength. However, as seen in Fig.10 (b), the phonon temperature evaluated by the temperature dependent electron-phonon coupling strength is rather higher than using the constant electron-phonon strength mainly after 300 fs. For femtosecond laser ablation, material damage usually occurs after the electron-phonon relaxation termination on timescale of picoseconds. So, it is important to use the temperature dependent electron-phonon coupling strength to predict ultrafast heating characteristics in multi-layer metal film assembly for target material ablation.

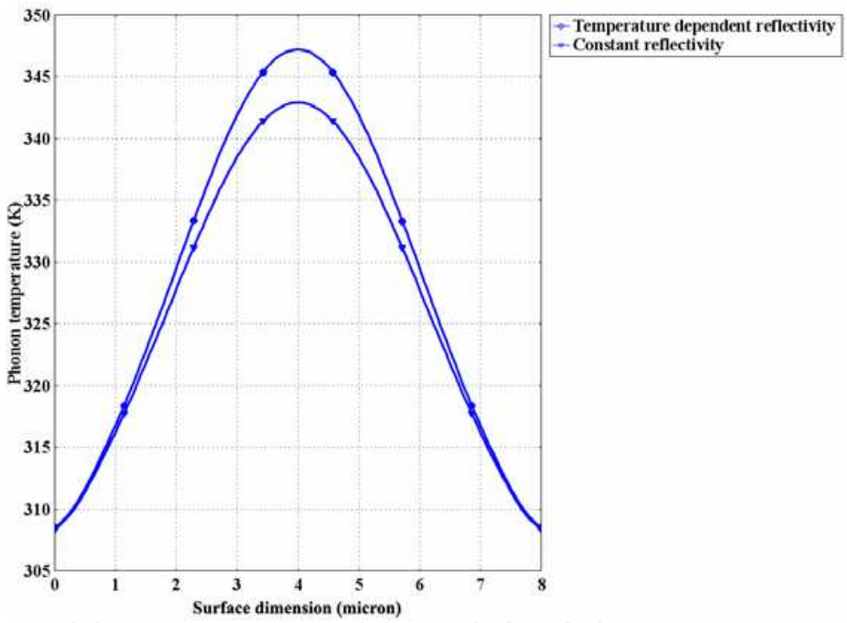

Fig. 11. The surface phonon temperature of the two layer Au/Al film assembly under the irradiation of laser spot at time of 15ps with respect to temperature dependent and constant reflectivity

The surface phonon temperature fields in the two layer Au/Al film assembly at 15 ps under range of laser spot with respect to the temperature dependent and the constant reflectivity are shown in Fig.11. The laser parameters are t_p=150 fs, F=0.05 J/cm^2, laser wavelength is 800 nm. It can be seen that the constant surface reflectivity definitely makes a low estimation of the surface phonon temperature, especially at center of the laser spot. The results can be explained as follows: When the femtosecond laser pulse irradiation on the target surface, the electron subsystem can be rapidly heated and the electron temperature is immediately evaluated to higher level during femtosecond laser pulse heating, causing dramatic increase of the total scattering rates. The large particle scattering rate is beneficial for reducing surface reflectivity as predicted by the Drude model with respect to temperature dependent

particle scattering processes. So the surface phonon temperature for the target with consideration of the temperature dependent reflectivity can be thus promoted as a result of reduction of the surface reflectivity for laser energy absorption by electron subsystem and the following energy coupling to phonon after the femtosecond laser pulse duration.

4. Conclusions

The ultrafast heating characteristics in the two layers and three layers metal film assemblies irradiated by femtosecond laser pulses are investigated by numerical simulations, in which the metals such as Au, Ag, Cu and Al are taken as the targets. The ultrafast 2-D temperature field evolutions on picosecond timescale with regard to the temperature dependent material properties for different film layer configurations of the multi-layer assemblies are obtained by Finite Element Method (FEM). The comparations for phonon temperature field evaluated by constant and temperature dependent electron-phonon coupling strength and reflectivity are given, which show the temperature dependent material properties must be taken into account for well exploring the ultrafast heating processes in multi-layer film assemblies. It is shown that the temperature field evolutions exhibit distinct characteristics for different layer configurations in the multi-layer assemblies. For the two layer Au/Ag assembly, the phonon temperature field is mainly distributed at the surface Au layer, while which can dominantly diffuse into the substrate layer for the Au/Al configuration after several picoseconds. Some similar results can also be observed in three layer metal film assemblies. It is demonstrated that electron-phonon coupling strength and phonon thermal capacity for the substrate layer play important roles in determining the temperature field distributions at the surface of Au coated assemblies. The increasing of second layer electron-phonon coupling strength and phonon thermal capacity both can result in severe drop of the surface Au layer phonon temperature. But, the electron thermal parameters including electron thermal conductivity and electron thermal capacity have less effect on the Au surface layer phonon temperature.

5. Acknowledgment

The work was supported by National High Technology R&D Program of China under the Grant No.2009AA04Z305 and National Science Foundation of China under the Grant No. 60678011.

6. References

Anisimov S., Kapeliovich B., and Perel'man T. (1974). Electron Emission from Metal Surfaces Exposed to Ultrashort Laser Pulses, *Sov. Phys. JETP,* Vol. 39, No. (August 1974),pp. 375-377.

Chen A.; Xu H.; Jiang Y.; Sui L.; Ding D.;Liu H. & Jin M. (2010). Modeling of Femtosecond Laser Damage Threshold on the Two-layer Metal Films. *Applied Surface Science,* Vol. 257, No.5, (December 2010),pp.1678-1683. ISSN 0169-4332

Chen J. & Beraun J. (2001).Numerical Study of Ultrashort Laser Pulse Interactions with Metal Films. *Numer. Heat Transfer A,* Vol. 40, No.1 (July 2001),pp. 1-20, ISSN 1040-7782

Chen J.; Tzou D.& Beraun J. (2006). A Semiclassical Two-temperature Model for Ultrafast Laser Heating. *International Journal of Heat and Mass Transfer*, Vol.49, No.1-2, (January 2006), pp.307-316.ISSN 0017-9310

Christensen B.; Vestentoft K. & Balling P. (2007). Short-pulse Ablation Rates and the Two Temperature Model. *Applied Surface Science,*Vol. 235, No.15, (May 2007),pp.6347-6352,ISSN 0169-4332

Kaganov M.; Lifshitz I.; & Tanatarov L.(1957). Relaxation Between Electrons and Crystalline Lattices. *Sov. Phys. JETP*, Vol. 4, No. 173, (1957),pp. 173-178

Kanavin A.; Smetanin I.; Isakov V.; Afanasiev Yu.; Chichkov B.; Wellegehausen B.; Nolte S.; Momma C. & Tünnermann A. (1998). Heat Transport in Metals Irradiated by Ultrashort Laser Pulses. *Physics. Review. B,* Vol.57, No.23, (June 1998),pp.14698-14703, ISSN 0163-1829

Liu K. (2007). Analysis of Thermal Behavior in Multi-layer Metal Thin Films Based on Hyperbolic Two-Step Model. *International Journal of Heat and Mass Transfer*,Vol.50,No.7-8, (April 2007), pp.1397-1407, ISSN 0017-9310

Qiu T.& Tien C. (1993). Heat Transfer Mechanisms During Short-Pulse Laser Heating of Metals, *ASME J. Heat Transfer*, Vol. 115, No.4,(November 1993), pp. 835-841, ISSN 0022-1481

Wang H.; Dai W.; Nassar R.& Melnik R. (2006).A Finite Difference Method for Studying Thermal Deformation in a Thin Film Exposed to Ultrashort-Pulsed Lasers. *International Journal of Heat and Mass Transfer*, Vol.49, No. 15-16, (July 2006),pp.2712-2723, ISSN 0017-9310

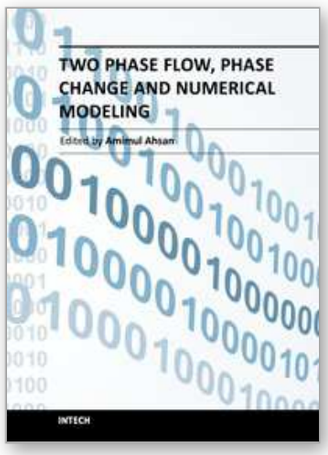

Two Phase Flow, Phase Change and Numerical Modeling
Edited by Dr. Amimul Ahsan

ISBN 978-953-307-584-6
Hard cover, 584 pages
Publisher InTech
Published online 26, September, 2011
Published in print edition September, 2011

The heat transfer and analysis on laser beam, evaporator coils, shell-and-tube condenser, two phase flow, nanofluids, complex fluids, and on phase change are significant issues in a design of wide range of industrial processes and devices. This book includes 25 advanced and revised contributions, and it covers mainly (1) numerical modeling of heat transfer, (2) two phase flow, (3) nanofluids, and (4) phase change. The first section introduces numerical modeling of heat transfer on particles in binary gas-solid fluidization bed, solidification phenomena, thermal approaches to laser damage, and temperature and velocity distribution. The second section covers density wave instability phenomena, gas and spray-water quenching, spray cooling, wettability effect, liquid film thickness, and thermosyphon loop. The third section includes nanofluids for heat transfer, nanofluids in minichannels, potential and engineering strategies on nanofluids, and heat transfer at nanoscale. The forth section presents time-dependent melting and deformation processes of phase change material (PCM), thermal energy storage tanks using PCM, phase change in deep CO2 injector, and thermal storage device of solar hot water system. The advanced idea and information described here will be fruitful for the readers to find a sustainable solution in an industrialized society.

How to reference
In order to correctly reference this scholarly work, feel free to copy and paste the following:

Feng Chen, Guangqing Du, Qing Yang, Jinhai Si and Hun Hou (2011). Ultrafast Heating Characteristics in Multi-Layer Metal Film Assembly Under Femtosecond Laser Pulses Irradiation, Two Phase Flow, Phase Change and Numerical Modeling, Dr. Amimul Ahsan (Ed.), ISBN: 978-953-307-584-6, InTech, Available from: http://www.intechopen.com/books/two-phase-flow-phase-change-and-numerical-modeling/ultrafast-heating-characteristics-in-multi-layer-metal-film-assembly-under-femtosecond-laser-pulses-

INTECH
open science | open minds

InTech Europe
University Campus STeP Ri
Slavka Krautzeka 83/A
51000 Rijeka, Croatia
Phone: +385 (51) 770 447
Fax: +385 (51) 686 166
www.intechopen.com

InTech China
Unit 405, Office Block, Hotel Equatorial Shanghai
No.65, Yan An Road (West), Shanghai, 200040, China
中国上海市延安西路65号上海国际贵都大饭店办公楼405单元
Phone: +86-21-62489820
Fax: +86-21-62489821

IntechOpen